How to cite: *Angew. Chem. Int. Ed.* **2022,** *61,* e202213953
International Edition: doi.org/10.1002/anie.202213953
German Edition: doi.org/10.1002/ange.202213953

Solar Cells

Singlet-Triplet Energy Gap as a Critical Molecular Descriptor for Predicting Organic Photovoltaic Efficiency

*Guangchao Han and Yuanping Yi**

Abstract: In contrast to the inorganic and perovskite solar cells, organic photovoltaics (OPV) depend on a series of charge generation and recombination processes, which complicates molecular design to improve the power conversion efficiencies (PCEs). Herein, we first propose the singlet-triplet energy gap (ΔE_{ST}) as a critical molecular descriptor for predicting the PCE considering that minimizing ΔE_{ST} is beneficial to simultaneously reduce voltage loss and triplet recombination. Remarkably, the results from data-driven machine learning verify that the prediction accuracy of the ΔE_{ST} (Pearson's correlation coefficient $r=0.72$) is apparently superior to that of two commonly used molecular descriptors in OPV, i.e., the optical gap ($r=0.65$) and the driving force ($r=0.53$). Moreover, an impressive prediction accuracy of $r=0.81$ is achieved just by combining the three descriptors. This work paves the way toward rapid and precise screening of efficient OPV materials.

Organic photovoltaics (OPV) is regarded as a promising renewable energy technology due to the advantages of light weight, flexibility, non-toxicity, and ease of fabrication. Benefitting from the emergence of A-D-A small-molecule nonfullerene acceptors (NFAs), the power conversion efficiencies (PCEs) have been rapidly promoted in recent years and surpassed 18% for single-junction devices.[1–6] Nonetheless, the OPV performance still lags behind the inorganic and perovskite solar cells. Thus, in order to realize high-throughput screening and rational design of efficient OPV materials, it is urgent to identify the most relevant molecular descriptors for the photovoltaic performance (Figure 1a). However, this is not straightforward because of OPV relying on a series of optoelectronic processes (Figure 1b). Furthermore, it remains challenging to quantify the correlation of the molecular descriptors with the PCE and the basic photovoltaic parameters, i.e., open-circuit voltage (V_{oc}), short-circuit current density (J_{sc}), and fill factor (FF).

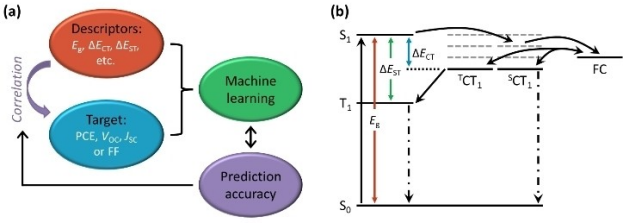

Figure 1. a) Illustration of the role of machine learning in the research of OPV. b) Diagram of excited-state energy levels and dynamics for the charge generation and recombination processes in OPV.

To seek the important descriptors for OPV, we revisit the key charge generation and recombination processes. Singlet excitons (S_1) firstly form upon light absorption and then diffuse to and dissociate at the donor/acceptor (D/A) interface into free carriers (FC) of holes and electrons, which subsequently migrate along the D and A materials toward and are finally extracted by the anode and cathode, respectively.[7–10] The photovoltaic optical gap (E_g), namely, the S_1 excitation energy of the narrow-band gap material, which is the threshold energy of absorbed photons, determines the upper limit of J_{sc}. The charge generation at the D/A interface consists of two steps: (1) dissociation of S_1 into the interfacial singlet charge-transfer state ($^SCT_1$) and (2) further separation of $^SCT_1$ into FC. The energy difference between the S_1 and $^SCT_1$ states that provides the CT driving force (ΔE_{CT}) is essential for charge generation and has an important impact on the J_{sc}. On the other hand, the requirement of ΔE_{CT} will lower the V_{oc} due to the decreased $^SCT_1$ energy and increased non-radiative (NR) voltage loss.[11–14] Therefore, the E_g and ΔE_{CT} are two important molecular descriptors and often used to predict the PCE according to the Scharber's model.[10,11,15–16] However, this famous model depends on the assumption of the key parameters, such as external quantum efficiency (determining J_{sc}), NR voltage loss (determining V_{oc}), and FF being empirical constants.

During charge migration, non-geminate recombination will result in the formation of CT excitons, with 25% singlet and 75% triplet ($^TCT_1$) manifolds according to the spin statistics. The $^TCT_1$ states can further relax to the lower-energy triplet excitons (T_1), mostly on the narrow-band gap materials, opening a major pathway of NR energy loss.[17–21] This jeopardizes the external quantum efficiency and V_{oc}. In competition with the extraction of charges, the recombina-

[*] Dr. G. Han, Prof. Y. Yi
Beijing National Laboratory for Molecular Sciences, CAS Key Laboratory of Organic Solids, Institute of Chemistry, Chinese Academy of Sciences
Beijing 100190 (China)
E-mail: ypyi@iccas.ac.cn
Prof. Y. Yi
University of Chinese Academy Sciences
Beijing 100049 (China)

tion to triplets will also reduce FF. Hence, suppressing the triplet recombination is critical to concurrently improve all the photovoltaic parameters. From the energetic point of view, the energy level of T_1 should be close to or higher than that of $^{T}CT_1$. Meanwhile, to ensure high V_{oc}, the ΔE_{CT} should be as small as possible. As a result, the singlet-triplet energy gap (ΔE_{ST}, i.e., the energy difference between S_1 and T_1) needs to be minimized.[22–25] To conclude, the ΔE_{ST} of the narrow-band gap materials is correlated closely with the triplet recombination and voltage loss, implying that it can be considered as an important molecular descriptor for OPV.

Herein, we demonstrated that the ΔE_{ST} is a critical molecular descriptor for predicting the PCE by the machine learning (ML) based on the database of 515 working OPV devices. Notably, the Pearson's correlation coefficient (r) is much superior for the ΔE_{ST} ($r=0.72$) with respect to the E_g ($r=0.65$) and ΔE_{CT} ($r=0.53$). Moreover, the combination of the three molecular descriptors yields a high r of 0.81, among the best prediction to date. In contrast with dozens of descriptors required in previous ML models,[26–33] the fewest descriptors are used here, which would benefit to rapidly screen high-performance OPV materials.[34–37]

To build reliable ML models, a database containing the three molecular properties (E_g, ΔE_{CT}, and ΔE_{ST}) and four primary photovoltaic parameters (V_{oc}, J_{sc}, FF, and PCE) was constructed. The values of E_g (determined by the onset of the absorption spectrum) and ΔE_{CT} (approximated to be the HOMO or LUMO energy offset between donor and acceptor, ΔE_{DA}) in the films are obtained from the available experiments. In order to take account of the aggregation effect, the solid-state ΔE_{ST} for the D and A materials (Table S1 and S2) were obtained by combining with theoretically calculated ΔE_{ST} of isolated molecules or polymer chains and experimentally measured E_g in the solutions and films (see Supporting Information for more details).[22,23] The database includes the results of both fullerene and nonfullerene OPV devices (Table S3 and S4). To minimize the influence of inferior active layer morphologies, the PCEs of all the chosen OPV devices should be higher than 4 % (Figure S1).

As a preliminary step, it is useful to make direct comparison between each two quantities of the three molecular descriptors and four photovoltaic parameters (Figure 2, S2, and S3). The calculated Pearson's correlation coefficients for all the pairs are shown in Figure 3. Both the ΔE_{DA} and ΔE_{ST} are moderately related to the E_g ($r=0.55$ and 0.57, respectively). The former can be ascribed to the small HOMO offsets often in the narrow-band gap A-D-A NFA based OPV devices. Consistent with the previous results,[27,38] the PCE is poorly correlated with the V_{oc} ($r=0.14$), but is closely correlated with the J_{sc} ($r=0.90$) and FF ($r=0.73$), indicating that regulating the molecular properties relevant to the J_{sc} and FF is important to improve the PCE. Apparently, all the three molecular properties are negatively correlated with the J_{sc} and PCE. As expected, the E_g exhibits a high correlation with the J_{sc} ($r=-0.78$). The negative correlation between the ΔE_{DA} and J_{sc} ($r=-0.47$) demonstrates that the ΔE_{DA} can be minimized without sacrificing charge generation.[39] Relatively, the ΔE_{ST} shows a weaker correlation with the J_{sc} ($r=-0.64$). Nevertheless, the correlation with the PCE is stronger for the ΔE_{ST} ($r=-0.64$)

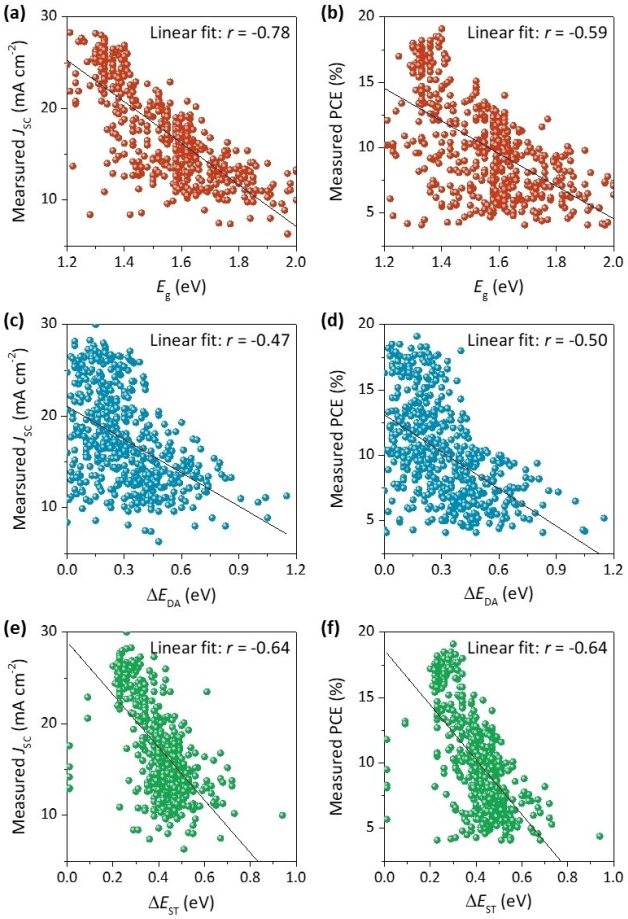

Figure 2. Measured J_{sc} and PCE versus E_g (a, b), ΔE_{DA} (c, d), and ΔE_{ST} (e, f).

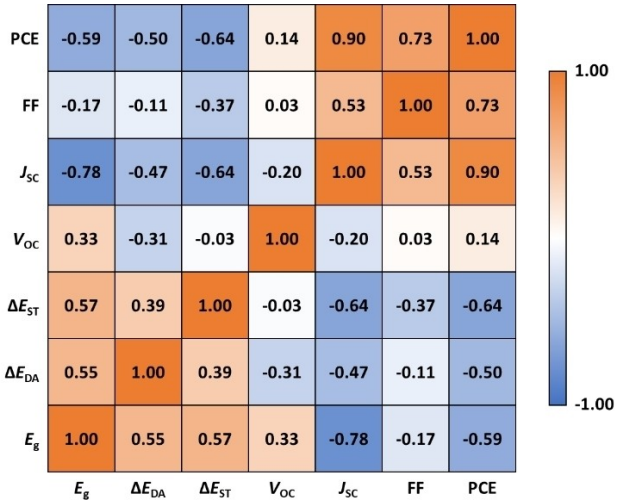

Figure 3. Pearson's correlation coefficients between each two quantities of the three molecular properties and four photovoltaic parameters.

than the E_g ($r=-0.59$). This can be ascribed to the more negative correlation of the ΔE_{ST} with the FF ($r=-0.37$) caused by the role of ΔE_{ST} in regulating triplet recombination.

Next, we established ML models with every one or two and all the three molecular descriptors to predict the four photovoltaic parameters. Three typical ML algorithms, namely, linear regression (LR), *k*-nearest neighbors (KNN), and gradient boosting regression tree (GBRT) were implemented by using the Scikit-Learn.[40] For each ML model, the leave-one-out (LOO) cross validation was carried out, with all data points except one as a training set to train the specific model and the remaining one as a test set to validate the model's prediction. The prediction accuracy is quantified by the Pearson's correlation coefficient, which was calculated by the predicted and actual values of each point in the test set for every LOO iteration. In most cases, GBRT performs slightly better than KNN and much better than the simplest LR (Table S5).[26] Hence, the GBRT results are used to analyze the underlying relationships.

The plots of GBRT predicted PCE with a single descriptor of the E_g, ΔE_{DA}, or ΔE_{ST} versus the measured J_{sc} or PCE are displayed in Figure 4. The prediction accuracy of J_{sc} using the E_g ($r=0.80$) or ΔE_{ST} ($r=0.74$) is higher than that using ΔE_{DA}. Remarkably, the prediction accuracy of PCE is evidently higher for the ΔE_{ST} ($r=0.72$) than for the E_g ($r=0.65$) and ΔE_{DA} ($r=0.53$), demonstrating that the ΔE_{ST} can be considered as a critical descriptor for predicting the PCE. In contrast, the prediction accuracies of V_{oc} and FF using a single descriptor are much poorer (Table S5). When using all the three molecular descriptors, the prediction accuracies are significantly increased. The improved accuracy of V_{oc} ($r=0.75$, Figure 5a) is primarily due to that the combination of E_g and ΔE_{DA}, which determines the CT_1 energy, has a good correlation with the V_{oc} ($r=0.70$). The descriptor importance for the GBRT model also indicates that the prediction of V_{oc} is dominated by the E_g and ΔE_{DA} (Figure 5e). We note that the importance of ΔE_{ST} is non-negligible, which can be attributed to the NR voltage loss caused by triplet recombination.[19,20] As expected, the high prediction accuracy for J_{sc} ($r=0.87$, Figure 5b) mainly depends on the E_g, and the ΔE_{ST} has a higher importance than the ΔE_{DA} (Figure 5e). Because of lacking of morphologically related descriptors, the prediction accuracy for FF ($r=0.44$, Figure 5c) remains not high, and the ΔE_{ST} exhibits the highest importance among the three descriptors (Figure 5e). Along with the improved prediction for V_{oc}, J_{sc} and

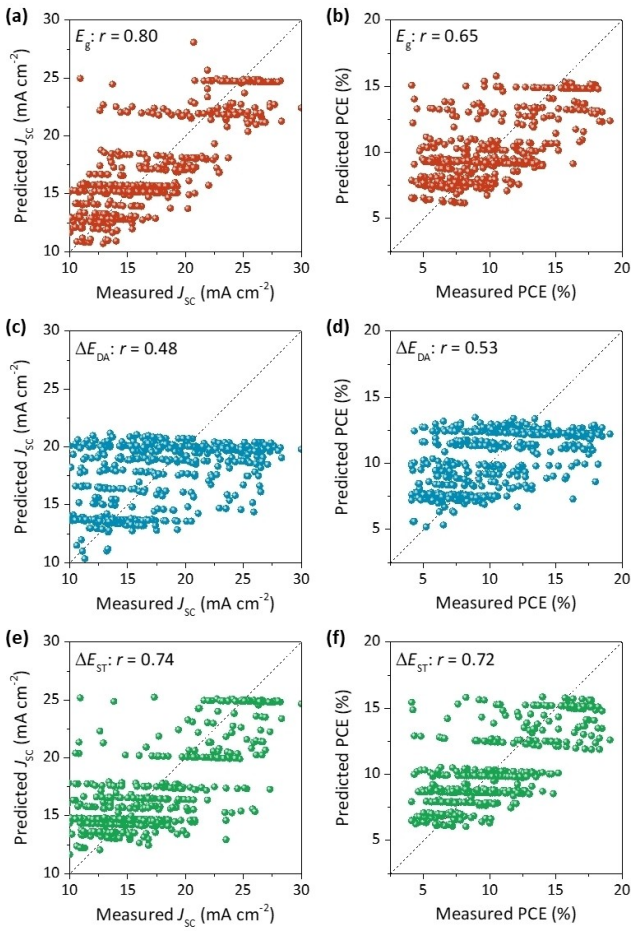

Figure 4. Predicted J_{sc} and PCE by GBRT with a single descriptor of E_g (a, b), ΔE_{DA} (c, d), or ΔE_{ST} (e, f) versus measured PCE and J_{sc}.

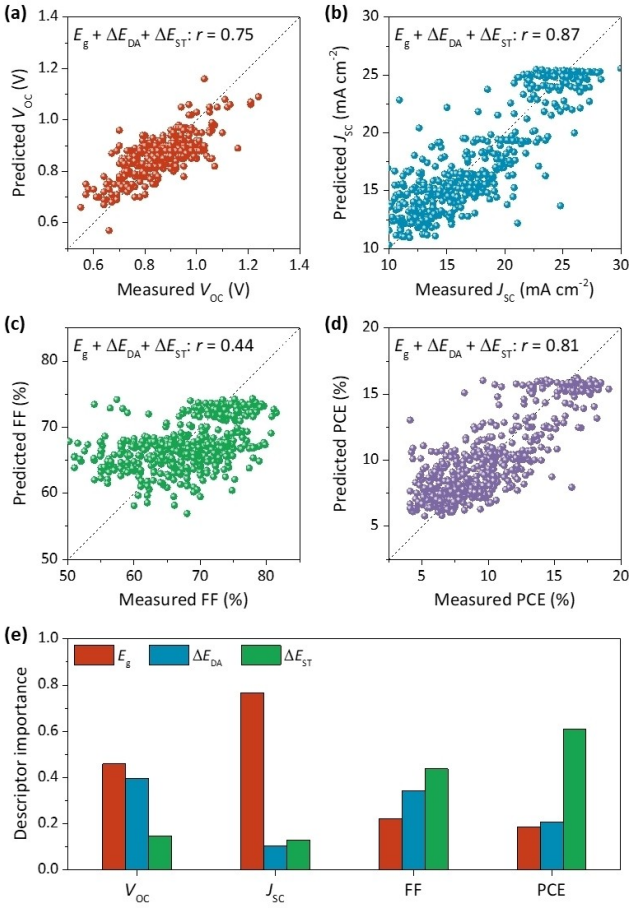

Figure 5. a–d) Predicted V_{oc}, J_{sc}, FF, and PCE by GBRT with all the three descriptors versus corresponding measured values. e) Descriptor Importance in the GBRT models.

FF, a prominent predictive performance is obtained for the PCE ($r=0.81$, Figure 5d). This is among the best PCE's prediction so far and only three descriptors are required,[26–33] which benefits for high-throughput screening of potential OPV candidates. Moreover, the importance of ΔE_{ST} is much higher than the other two descriptors (Figure 5e), confirming that the ΔE_{ST} is critical to determine the PCE.

Finally, it is imperative to discuss how to effectively reduce the ΔE_{ST} for designing high-performance OPV materials. A common strategy is maximizing the intramolecular CT effect (i.e., minimizing the overlap between the HOMO and LUMO wavefunctions), which has been successfully used to design thermally activated decay fluorescence molecules for highly efficient organic light-emitting diodes.[41,42] Figure S4 shows the chemical structures and frontier molecular orbitals of three representative OPV polymers (P3HT, PffBT4-2OD, and N2200). As the intramolecular CT effect gets stronger from P3HT to PffBT4T-2OD and to N2200, the calculated ΔE_{ST} is substantially decreased (Figure 6a). In particular, the vertical (adiabatic) ΔE_{ST} for N2200 is as small as 0.2 (0.01) eV. Nevertheless, the much reduced HOMO–LUMO overlap will inevitably result in small oscillator strength (f) for the S_1 state and weak light absorption, which is adverse to realizing high J_{sc} and limits the PCEs of N2200-based OPV devices within 12 %.[43,44] Interestingly, owing to modest intramolecular CT effect, A-D-A NFAs exhibit moderate ΔE_{ST} (e.g., 0.4–0.5 eV for ITIC, IT-4F, and Y6) and large f ($\approx$3) in the isolated molecules. Furthermore, end-group π-π stacking, which are frequently present in the films, can decrease the ΔE_{ST} to $\approx$0.3 eV without sacrificing f (Figure 6a). Thus, the A-D-A NFAs have both strong light absorption and relatively small ΔE_{ST}.[23,24] This is responsible for the high J_{sc} and FF in the low-driving-force NF OPV devices.[1–6]

In summary, the ΔE_{ST} is proposed as an effective molecular descriptor to predict the OPV PCE in view of the crucial role of ΔE_{ST} in controlling the charge generation and recombination processes. The data-driven machine-learning results verify that the PCE exhibits evidently higher correlation with the ΔE_{ST} ($r=0.72$) than the two conventional descriptors, E_g ($r=0.65$) and ΔE_{DA} ($r=0.53$). Because enhancing the intramolecular CT effect can reduce both the oscillator strength and S_1 energy and the end-group π–π stacking reduced ΔE_{ST} comes mostly from the decreased S_1 energy (Figure 6b), the ΔE_{ST}, to some extent, is linearly correlated to the E_g ($r=0.57$). Moreover, because the weakly bound polaron pairs formed in strong D–A copolymers can be regarded as the precursor of free charge carriers, the ΔE_{ST} can be also relevant to charge generation.[45–47] Consequently, the ΔE_{ST} is associated with the oscillator strength, E_g, and charge generation in an indirect way, thus increasing the prediction for J_{sc} ($r=0.74$) and PCE. Remarkably, the combination of ΔE_{ST}, E_g, and ΔE_{DA} results in the prediction accuracy as high as 0.81, which is among the best PCE prediction. Although the evaluation of the three descriptors here relies on syntheses and experimental absorption spectra and energy levels, this work could open an avenue to high-throughput screening of new OPV materials considering efficient computational approaches being actively developed to calculate these parameters in the solid state.[39]

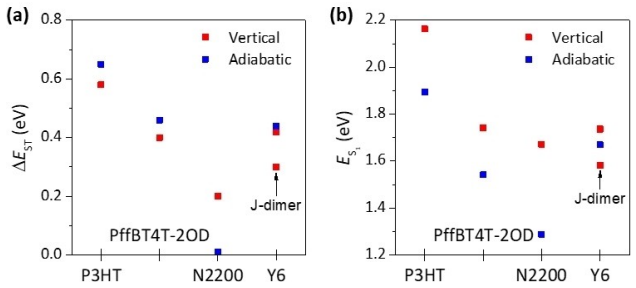

Figure 6. Calculated vertical and adiabatic ΔE_{ST} (a) and S_1 energies (b) for P3HT, PffBT4T-2OD, N2200, and Y6.

Acknowledgements

The work is financially supported by the National Natural Science Foundation of China (Grant No. 22173108 and 91833305).

Conflict of Interest

The authors declare no conflict of interest.

Data Availability Statement

The data that support the findings of this study are available in the supplementary material of this article.

Keywords: Energy Gap · Machine Learning · Singlet-Triplet · Solar Cells · Triplet Recombination

[1] C. Yan, S. Barlow, Z. Wang, H. Yan, A. K. Y. Jen, S. R. Marder, X. Zhan, *Nat. Rev. Mater.* **2018**, *3*, 18003.
[2] G. Zhang, J. Zhao, P. C. Y. Chow, K. Jiang, J. Zhang, Z. Zhu, J. Zhang, F. Huang, H. Yan, *Chem. Rev.* **2018**, *118*, 3447.
[3] Q. Liu, Y. Jiang, K. Jin, J. Qin, J. Xu, W. Li, J. Xiong, J. Liu, Z. Xiao, K. Sun, S. Yang, X. Zhang, L. Ding, *Sci. Bull.* **2020**, *65*, 272.
[4] W. Liu, X. Xu, J. Yuan, M. Leclerc, Y. Zou, Y. Li, *ACS Energy Lett.* **2021**, *6*, 598.
[5] C. Li, J. Zhou, J. Song, J. Xu, H. Zhang, X. Zhang, J. Guo, L. Zhu, D. Wei, G. Han, J. Min, Y. Zhang, Z. Xie, Y. Yi, H. Yan, F. Gao, F. Liu, Y. Sun, *Nat. Energy* **2021**, *6*, 605.
[6] Y. Cui, Y. Xu, H. Yao, P. Bi, L. Hong, J. Zhang, Y. Zu, T. Zhang, J. Qin, J. Ren, Z. Chen, C. He, X. Hao, Z. Wei, J. Hou, *Adv. Mater.* **2021**, *33*, 2102420.
[7] J.-L. Brédas, J. E. Norton, J. Cornil, V. Coropceanu, *Acc. Chem. Res.* **2009**, *42*, 1691.
[8] T. M. Clarke, J. R. Durrant, *Chem. Rev.* **2010**, *110*, 6736.
[9] G. Han, Y. Yi, Z. Shuai, *Adv. Energy Mater.* **2018**, *8*, 1702743.
[10] G. Han, Y. Yi, *Adv. Theory Simul.* **2019**, *2*, 1900067.

[11] J. Benduhn, K. Tvingstedt, F. Piersimoni, S. Ullbrich, Y. Fan, M. Tropiano, K. A. McGarry, O. Zeika, M. K. Riede, C. J. Douglas, S. Barlow, S. R. Marder, D. Neher, D. Spoltore, K. Vandewal, *Nat. Energy* **2017**, *2*, 17053.
[12] D. Qian, Z. Zheng, H. Yao, W. Tress, T. R. Hopper, S. Chen, S. Li, J. Liu, S. Chen, J. Zhang, X.-K. Liu, B. Gao, L. Ouyang, Y. Jin, G. Pozina, I. A. Buyanova, W. M. Chen, O. Inganäs, V. Coropceanu, J.-L. Bredas, H. Yan, J. Hou, F. Zhang, A. A. Bakulin, F. Gao, *Nat. Mater.* **2018**, *17*, 703.
[13] F. D. Eisner, M. Azzouzi, Z. Fei, X. Hou, T. D. Anthopoulos, T. J. S. Dennis, M. Heeney, J. Nelson, *J. Am. Chem. Soc.* **2019**, *141*, 6362.
[14] G. Han, Y. Yi, *J. Phys. Chem. Lett.* **2019**, *10*, 2911.
[15] M. C. Scharber, D. Mühlbacher, M. Koppe, P. Denk, C. Waldauf, A. J. Heeger, C. J. Brabec, *Adv. Mater.* **2006**, *18*, 789.
[16] M. C. Scharber, *Adv. Mater.* **2016**, *28*, 1994.
[17] A. Rao, P. C. Y. Chow, S. Gélinas, C. W. Schlenker, C.-Z. Li, H.-L. Yip, A. K. Y. Jen, D. S. Ginger, R. H. Friend, *Nature* **2013**, *500*, 435.
[18] S. M. Menke, A. Sadhanala, M. Nikolka, N. A. Ran, M. K. Ravva, S. Abdel-Azeim, H. L. Stern, M. Wang, H. Sirringhaus, T.-Q. Nguyen, J.-L. Brédas, G. C. Bazan, R. H. Friend, *ACS Nano* **2016**, *10*, 10736.
[19] A. J. Gillett, A. Privitera, R. Dilmurat, A. Karki, D. Qian, A. Pershin, G. Londi, W. K. Myers, J. Lee, J. Yuan, S.-J. Ko, M. K. Riede, F. Gao, G. C. Bazan, A. Rao, T.-Q. Nguyen, D. Beljonne, R. H. Friend, *Nature* **2021**, *597*, 666.
[20] Z. Chen, X. Chen, Z. Jia, G. Zhou, J. Xu, Y. Wu, X. Xia, X. Li, X. Zhang, C. Deng, Y. Zhang, X. Lu, W. Liu, C. Zhang, Y. Yang, H. Zhu, *Joule* **2021**, *5*, 1832.
[21] R. Wang, J. Xu, L. Fu, C. Zhang, Q. Li, J. Yao, X. Li, C. Sun, Z.-G. Zhang, X. Wang, Y. Li, J. Ma, M. Xiao, *J. Am. Chem. Soc.* **2021**, *143*, 4359.
[22] D. Veldman, S. C. J. Meskers, R. A. J. Janssen, *Adv. Funct. Mater.* **2009**, *19*, 1939.
[23] G. Han, T. Hu, Y. Yi, *Adv. Mater.* **2020**, *32*, 2000975.
[24] J. P. A. Souza, L. Benatto, G. Candiotto, L. S. Roman, M. Koehler, *J. Phys. Chem. A* **2022**, *126*, 1393.
[25] S. Pang, Z. Wang, X. Yuan, L. Pan, W. Deng, H. Tang, H. Wu, S. Chen, C. Duan, F. Huang, Y. Cao, *Angew. Chem. Int. Ed.* **2021**, *60*, 8813; *Angew. Chem.* **2021**, *133*, 8895.
[26] H. Sahu, W. Rao, A. Troisi, H. Ma, *Adv. Energy Mater.* **2018**, *8*, 1801032.
[27] H. Sahu, H. Ma, *J. Phys. Chem. Lett.* **2019**, *10*, 7277.
[28] D. Padula, J. D. Simpson, A. Troisi, *Mater. Horiz.* **2019**, *6*, 343.
[29] M.-H. Lee, *Adv. Energy Mater.* **2019**, *9*, 1900891.
[30] Z.-W. Zhao, M. del Cueto, Y. Geng, A. Troisi, *Chem. Mater.* **2020**, *32*, 7777.
[31] Y. Miyake, A. Saeki, *J. Phys. Chem. Lett.* **2021**, *12*, 12391.
[32] K. Kranthiraja, A. Saeki, *Adv. Funct. Mater.* **2021**, *31*, 2011168.
[33] A. Mahmood, J.-L. Wang, *Energy Environ. Sci.* **2021**, *14*, 90.
[34] A. Mahmood, J.-L. Wang, *J. Mater. Chem. A* **2021**, *9*, 15684.
[35] A. Mahmood, A. Irfan, J.-L. Wang, *J. Mater. Chem. A* **2022**, *10*, 4170.
[36] A. Mahmood, A. Irfan, J.-L. Wang, *Chem. Eur. J.* **2022**, *28*, e202103712.
[37] Z.-W. Zhao, Ö. H. Omar, D. Padula, Y. Geng, A. Troisi, *J. Phys. Chem. Lett.* **2021**, *12*, 5009.
[38] N. E. Jackson, B. M. Savoie, T. J. Marks, L. X. Chen, M. A. Ratner, *J. Phys. Chem. Lett.* **2015**, *6*, 77.
[39] G. Han, Y. Yi, *Acc. Chem. Res.* **2022**, *55*, 869.
[40] F. Pedregosa, G. Varoquaux, A. Gramfort, V. Michel, B. Thirion, O. Grisel, M. Blondel, P. Prettenhofer, R. Weiss, V. Dubourg, J. Vanderplas, A. Passos, D. Cournapeau, M. Brucher, M. Perrot, É. Duchesnay, *J. Mach. Learn. Res.* **2011**, *12*, 2825.
[41] H. Uoyama, K. Goushi, K. Shizu, H. Nomura, C. Adachi, *Nature* **2012**, *492*, 234.
[42] X.-K. Chen, D. Kim, J.-L. Brédas, *Acc. Chem. Res.* **2018**, *51*, 2215.
[43] Z. Li, L. Ying, P. Zhu, W. Zhong, N. Li, F. Liu, F. Huang, Y. Cao, *Energy Environ. Sci.* **2019**, *12*, 157.
[44] L. Zhu, W. Zhong, C. Qiu, B. Lyu, Z. Zhou, M. Zhang, J. Song, J. Xu, J. Wang, J. Ali, W. Feng, Z. Shi, X. Gu, L. Ying, Y. Zhang, F. Liu, *Adv. Mater.* **2019**, *31*, 1902899.
[45] B. S. Rolczynski, J. M. Szarko, H. J. Son, Y. Liang, L. Yu, L. X. Chen, *J. Am. Chem. Soc.* **2012**, *134*, 4142.
[46] R. Tautz, E. Da Como, T. Limmer, J. Feldmann, H.-J. Egelhaaf, E. von Hauff, V. Lemaur, D. Beljonne, S. Yilmaz, I. Dumsch, S. Allard, U. Scherf, *Nat. Commun.* **2012**, *3*, 970.
[47] R. Wang, Y. Yao, C. Zhang, Y. Zhang, H. Bin, L. Xue, Z.-G. Zhang, X. Xie, H. Ma, X. Wang, Y. Li, M. Xiao, *Nat. Commun.* **2019**, *10*, 398.

Manuscript received: September 21, 2022
Accepted manuscript online: October 11, 2022
Version of record online: November 9, 2022